### PARTICLE TECHNOLOGY AND FLUIDIZATION





# Discrete element method simulation of binary blend mixing of cohesive particles in a high-intensity vibration system

Kai Zheng | Kuriakose Kunnath | Rajesh N. Davé 🗅

Chemical and Materials Engineering Department, New Jersey Institute of Technology, Newark, New Jersey, USA

#### Correspondence

Rajesh N. Davé, New Jersey Center for Engineered Particulates, New Jersey Institute of Technology, Newark, NJ 07102, USA. Email: dave@njit.edu

#### **Funding information**

National Science Foundation, Grant/Award Number: IIP-1919037

#### **Abstract**

The effects of processing intensity, time, and particle surface energy on mixing of binary cohesive powder blends in high-intensity vibration system were investigated via discrete element method simulations. The mixedness was quantified by the coefficient of variation,  $C_v$ ; lower being better. The mixing rate, which is the speed at which homogeneity was achieved, was inversely proportional to the mixing Bond number, defined as the ratio of particle cohesion to the shear force resulting from the mixing intensity. Results show that both increasing processing intensity and reducing surface energy led to a faster mixing rate. However, the mixedness improved initially as mixing action (the product of mixing rate and mixing time) increased, but later deteriorated upon its further increase. Thus, both mixing rate and mixing intensity need to be tuned for optimum mixing performance depending on the cohesion level of particles; too high or too low mixing action should be avoided.

## KEYWORDS

wileyonlinelibrary.com/journal/aic

cohesive particle mixing, DEM simulation, mixing bond number, mixing mechanism

#### **INTRODUCTION** 1

The mixing of powders is a common but important step in chemical, mining, pharmaceutical, food, and other industries. 1-6 The aim of mixing is to produce a mixture with adequate homogeneity, despite potential variations in powder properties such as particle size, particle-size distribution, density, flowability, surface characteristics. Processing conditions, such as the equipment, and operating conditions, as well as the upstream and downstream processing steps, can also vary. 4,6-11 For example, in a continuous direct compression tableting process, blend and drug content uniformity after feeding and mixing are critical factors for meeting tablet product uniformity requirements. 12-14 In addition to particle size disparities between the constituents, the flowability of the powders is expected to have a critical impact on degree of mixing or segregation. 4,14-16 Existing literature provides the phenomenological explanations as well as some model-based understanding of particle mixing behavior. 1,3,17-19 Factors such as the particle density, particle sizes, size ratio, surface roughness, surface energy, and shear rate, have been considered in analyzing the interactions between particles. 6,20-23 In general, the current understanding suggests that as compared with noncohesive powders, cohesive blends are less likely to segregate although they may pose some challenges in achieving the mixing homogeneity, possibly requiring devices with higher intensity or longer processing times. Unfortunately, there is limited understanding of the device effect and/or the mixing intensity effect.

There are a variety of mixers available, and several different ones have been used for dry mixing of powders. 4,24-29 Most industrial mixing devices exert relatively low intensity in comparison to those used in creating interactive mixtures. 4,14,23 Generally, low-intensity blenders such as a tumbling blender, V-blender, Turbula mixer, ribbon blender, etc., are used in various industrial mixing applications. 30,31 For some of these, their effective mixing action may be considered high intensity at larger industrial scale. However, for the purpose of achieving higher intensity at lab-scale, high-intensity mixing devices may be required. For example, vibrational mixers may be used as they have attracted attention due to their fast-mixing rate and good mixing quality. 32,33 In addition to processing conditions, the degree of mixing attained in a mixer is also likely to be significantly affected by particle properties such as size, shape, and cohesion, because the rate and

degree of mixing of free-flowing spherical particles are much higher than that of cohesive irregular particles.<sup>2,4,5,27</sup> Unfortunately, the selection of mixing devices and processing parameters based on particle cohesion remains an underexplored topic. Therefore, further research is required to develop better understanding of mixing mechanisms for the cohesive fine powders. Establishing relationships between mixing quality and particle properties together with processing conditions may benefit academics and industry practitioners in predicting mixing performance and selecting processing conditions for their specific applications.

Since the detailed experimental analysis of particle dynamics is rather challenging, discrete element method (DEM) modeling and simulations have been widely used because they allow for the computation of translational and rotational motion of individual particles in the system, which helps obtain detailed diagnostics of a process. 6,9,34-36 Likewise, DEM simulations have been used to uncover macroscopic behavior of particulate matter. 6,27,37,38 DEM has also been used effectively to study the mixing process of free-flowing particles. 39-41 However, the investigation of mixing mechanisms of cohesive particles through DEM simulations has been less explored; only a few examples of DEM simulations dealing with cohesive particles can be found in the literature. 11,42 In those studies, the selected range of cohesive forces was relatively narrow, making it difficult to gain a general understanding of the effect of particle cohesion on the mixing process.<sup>36</sup> Nonetheless, DEM simulations are attractive as compared to traditional physical experiments, with which it is rather challenging to develop general understanding due to the different mixing mechanisms and energy inputs of various mixing devices. Therefore, DEM simulations are utilized as an alternative to experimental investigation for understanding the effect of cohesion on the mixing process, which could potentially help select processing conditions.9

In this article, the cohesive powder mixing process in a highintensity vibrational mixing system was investigated via DEM simulation, keeping fine powder blending as the application of relevance. The objective is to develop a better mechanistic understanding of the mixing process by analyzing the relative effects of cohesion originating from particle surface energy and shearing forces due to mixing intensity. Mixing intensity was varied by applying different vibrational conditions, and particle cohesion was varied via surface energy of the particles. The mixing process was analyzed by computing collision shear forces, collision numbers, and nature of the collisions, as well as resulting powder bed porosity. The mixing Bond number, (Bom), was introduced to characterize the mixing behavior, and is defined as the ratio of pull-off force, which represents the particle cohesion, to the shear force resulting from the mixing intensity. The effective mixing rate  $(R_m)$  was used to evaluate the speed at which a mixture reaches homogeneity. Bo<sub>m</sub> was used as one of two important factors, the second one being the mixing time, to estimate the effective mixing rate. In the remainder of the article, the effective mixing rate will be termed "the mixing rate," with higher values corresponding to higher mixing rate. The coefficient of variation of the mixture  $(C_v)$ , which has been frequently used for the characterization of fine powder mixture such as pharmaceutical blends, was used

to represent the mixing quality. Meanwhile, the mixing action  $(P_{r,t})$  was captured through the product of *effective* mixing rate  $(R_m)$  and mixing time. Simulations were performed to examine the effect of  $P_{r,t}$  on the mixing quality  $(C_v)$ . Thus, it is hoped that  $P_{r,t}$  could be used to understand the effect of mixing intensity and processing time on the cohesive particle mixture quality and mixing dynamics.

# 2 | SIMULATED SYSTEM AND BLEND CONTENT UNIFORMITY

#### 2.1 | DEM simulation approach

A commercial DEM simulation package named EDEM (EDEM 2018, DEM Solutions) was used to investigate the cohesive particle mixing process in a high-intensity vibration system. Translational and rotational motion of individual particles are calculated by the following equations.

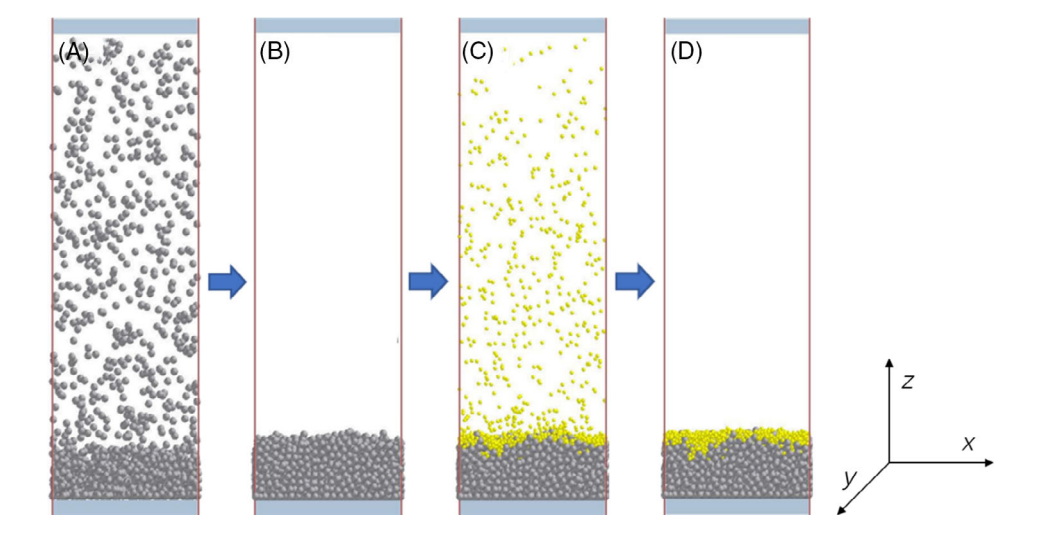
$$m_i \frac{d\vec{v}_i}{dt} = \vec{F}_i + m_i \vec{g}. \tag{1}$$

$$I_i \frac{d\vec{\omega}_i}{dt} = \vec{\mathsf{T}}_i. \tag{2}$$

In Equation (1),  $m_i$ ,  $\vec{v}_i$ , t,  $\vec{g}$ , and  $\vec{F}_i$  are the mass of particle i, velocity vector of particle i, time, gravitational acceleration, and contact forces for the particle-particle and particle-geometry interactions, respectively. In Equation (2),  $I_i$ ,  $\vec{\omega}_i$ , and  $\vec{T}_i$  are the moment of inertia, angular velocity, and torque acting on particle i, which are induced by tangential contact force and rolling friction, respectively. Hertz-Mindlin with Johnson-Kendall-Roberts (JKR) cohesion contact model was used to describe the interparticle interaction between particles and interaction between particle-vessel geometry. 43,44 The JKR force model with Hertz contact model assumes that the total contact force is the sum of elastic Hertzian contact force and van der Waals forces representing adhesion between two contact areas, and using calculated via surface energy and particle size values. 45,46 The model has been proven to be a time-tested method to investigate the strongly adhesive particle system and has been used and reported in many publications. 27,46-48 Therefore, the same approach, employing the JKR force model with the Hertz contact model, was used in this work.

In order to simulate the cohesive particle mixing process, two sets of mono-sized particles were generated in a cuboid container with length, width, and height of 1, 1, and 3 cm, respectively. As shown in Figure 1, 3000 large particles (gray) with 500  $\mu m$  diameter were randomly generated and settled down at the bottom of container first, and then fine particles (yellow) with 250  $\mu m$  diameter were randomly generated and allowed to settle down on the top of coarse particles. A 10% by weight of fine particles are used in this simulation study. After coarse and fine particles were introduced, the container vibrated at a pre-set amplitude from 5 to

**FIGURE 1** Snapshots at various simulation times. (A) Simulation time = 0.1 s, (B) simulation time = 0.25 s, (C) simulation time = 0.5 s, (D) simulation time = 0.75 s



10 mm with a frequency of 60 Hz along the z direction, thus having effective accelerations of 50 times gravity (Gs) and 100 Gs, $^{49}$  respectively.

When cohesive force is much higher than a particle's weight, due to fine particle sizes or high van der Waals, electrostatic, or capillary forces, the mixing performance will be significantly affected.<sup>4</sup> Such an effect can be captured through a dimensionless parameter called the granular Bond number, defined as the ratio of cohesive force to gravity, and widely used to quantify interparticle cohesion.<sup>20,37,50</sup> It is given by the following expression,

$$Bo_g = \frac{F_{\text{cohesion}}}{mg},\tag{3}$$

where  $F_{\text{cohesion}}$  is the interparticle cohesive force acting on a particle, m is the mass of the particle, and g is the acceleration of gravity. In the JKR model, the normal cohesive force depends on the overlap ( $\delta$ ) and the interaction parameter, surface energy ( $\gamma$ ), given by the following equations,

$$F_{JKR} = \frac{4E^*}{3R_e} a^3 - 4\sqrt{\pi \gamma E^*} a^{\frac{3}{2}}, \tag{4}$$

$$a^{4}-2R_{e}\delta a^{2}-\frac{2\pi w}{E^{*}}R_{e}^{2}a+R_{e}^{2}\delta^{2}=0, \tag{5} \label{5}$$

$$\frac{1}{R_0} = \frac{1}{r_1} + \frac{1}{r_1},\tag{6}$$

$$E^* = \left(\frac{1 - v_i^2}{E_i} + \frac{1 - v_j^2}{E_j}\right)^{-1},\tag{7}$$

where a is the contact radius,  $R_e$  and  $E^*$  are equivalent radius and combined elastic modulus, respectively, and  $v_i$ ,  $v_j$ ,  $E_i$ ,  $E_j$  represent the Poisson's ratios, and Young's moduli of particles i and j. The maximum value of cohesion force occurs when particles break physical contact

with each other. The value of maximum cohesion force, called pull-off force, is given by

$$F_{\text{pull off}} = -\frac{3}{2}\pi\gamma R_e. \tag{8}$$

In this study, the pull-off force is considered as the representative cohesive force. Although this simulation employs larger particles for the sake of keeping the computational burden limited, it was intended to mimic the experimental system comprising of coarse acetaminophen and Avicel 101 with sizes of 20 and 45 µm and surface energies of 40.86 and 42.33 mJ/m<sup>2</sup>, respectively.<sup>33</sup> To avoid excessive computational burden, while retaining the relevant physics of the real particulate system, the surface energy values and particle sizes were accounted for by ensuring that the Bond numbers of simulated particles were similar to the real ones. 51 This strategy was implemented to account for the effects of cohesion for larger simulated particle sizes. The Bond number, which is the ratio of cohesive force to body or gravitational force, was used as a scaling parameter and is a strong function of both the particle size and surface energy, as described in Equation (3). The actual Bond number of coarse acetaminophen and Avicel 101 are  $1.4 \times 10^6$  and  $2.6 \times 10^5$ , respectively. Here, two standard model particles with the particle sizes of 250 and 500 µm, respectively, and surface energy values of 5 J/m<sup>2</sup> were used. Thus, the simulated system Bond numbers for fine and coarse particles calculated using Equations (3)-(8) are  $1.1 \times 10^6$  and  $2.7 \times 10^5$ , respectively. Therefore, notwithstanding the limitations of the Bond number scaling strategy, the mixing performance of coarse Acetaminophen and Avicel 101 can be reasonably simulated and captured. In summary, as compared with previous work utilizing DEM,6,52 simulated particles sizes were finer and surface energy was adjusted to impart the required level of cohesion. Other than particle size, the material properties of all particles were held constant for each simulation and are listed in Table 1. The ratio of coarse to fine particle size was fixed at 2, so that the size-driven effect on mixing was neither too small nor too high.6

**TABLE 1** Initial parameters and material properties used in the simulation

Parameter	Value	Unit
Density of coarse particle	1.65	g/ml
Diameter of coarse particle	500	μm
Shear modulus of coarse particle	$4 \times 10^9$	Pa
Poisson ratio of coarse particle	0.25	-
Number of coarse particles	3000	-
Density of fine particle	1.65	g/ml
Diameter of fine particle	250	μm
Shear modulus of fine particle	$4 \times 10^9$	Pa
Poisson ratio of fine particle	0.25	-
Number of fine particles	2664	-
Density of vessel	2500	kg/m <sup>3</sup>
Shear modulus of vessel	$4 \times 10^9$	Pa
Poisson ratio of vessel	0.25	-
Length of vessel	10	mm
Width of vessel	10	mm
Height of vessel	30	mm
Frequency of vibration	60	Hz
Time step	$3.0\times10^{-8}$	S

Particle-particle sliding/rolling frictions and Young's modulus can also affect the performance of cohesive powders during mixing. 46,53,54 However, most previous works considered noncohesive, larger (>5 mm) particles. 46,53 For such cases, the particle interactions such as friction are expected to dominate the interaction between particles. In contrast, the impact of Young's modulus and friction is expected to be lower compared to other major drivers, such as cohesive forces and wall effects, when the particles are fine and cohesive. Here, the emphasis is on numerical investigation on the topic of mixing of cohesive powders, and impact of the primary factors such as the surface energy, mixing intensity, and process intensity. Here, periodic boundary conditions (PBCs) were used so the sidewall effects and particle-wall sliding/rolling friction effects are reduced on the mixing process. Although it is likely that such effects could be relevant, the current study is expected to capture the influence of key parameters so as to provide the outcomes that are of practical relevance for cohesive powder mixing affected by powder cohesion. In addition, the domain of the PBC is such that the shortest dimension is at least 20 times the coarse particle diameter, or 40 times the fine particle diameter. That could limit the impact of the vessel dimensions on potential segregation. Future investigations can also emphasize other potential drivers, such as Young's modulus and friction, that have been found to affect granular segregation. 53,55

### 2.2 | Quantification of content uniformity

Powder blend homogeneity is a key factor used to evaluate the mixing quality after processing. As shown in Figure 2, the mixture was initially allowed to settle down at the bottom of container and this region was

divided into 10 zones along the vertical axis for the sake of mixing quality quantification. The coefficient of variation ( $C_v$ ) of the concentration of fine particles (yellow) in each zone was computed as below.

$$C_v = \frac{\text{Standard deviation of concentration of fine particles in each zone}}{\text{Average concentration of fine particles in the mixture}}.$$

The *Johnson* model, which is an excellent model for predicting theoretical  $C_v$  values of ideal mixing of two components based on dosage and particle-size distribution, is considered.<sup>56</sup> The  $C_v$  value for the Johnson model is given by the following expression.

$$C_{v} = 100y \left(\frac{500\pi\rho}{3G}\right)^{0.5} \left[\sum f_{i} \left(\frac{d_{i}}{10,000}\right)^{3}\right]^{0.5}.$$
 (10)

Here, y is the fraction of major component in the mixture, which is 0.9 in this study,  $\rho$  is the true density of the drug (g/ml), G is the fine particle dose per sample (mg). Here, it is the total mass (36 mg) of all n number of fine particles, calculated as  $G = \frac{1}{4}n\pi d_i^2 \rho$ ,  $d_i$  is the mean particle size ( $\mu$ m),  $f_i$  is the weight fraction of the mean particle size  $d_i$  ( $\mu$ m).

In this study,  $C_v$  value is a nondimensional parameter. Hence percentage (%) is used to show the mixing homogeneity or quality. If the actual  $C_v$  value is close to or lower than the theoretical  $C_v$  value based on the *Johnson* model, the mixture is considered well mixed. Otherwise, the mixing quality is inadequate and further mixing time is needed to reach homogeneity. It should be noted that the theoretical well-mixing  $C_v$  value is relatively high in this study which is due to the fine dosage of sample and coarse particle size.

### 2.3 | Mixing performance

In this study, mixing performances were evaluated by the effective mixing rate, collision rate, and mixing Bond number. The effective mixing rate ( $R_m$ ) was assessed to understand the particle mixing behavior and can be calculated using the equation below.

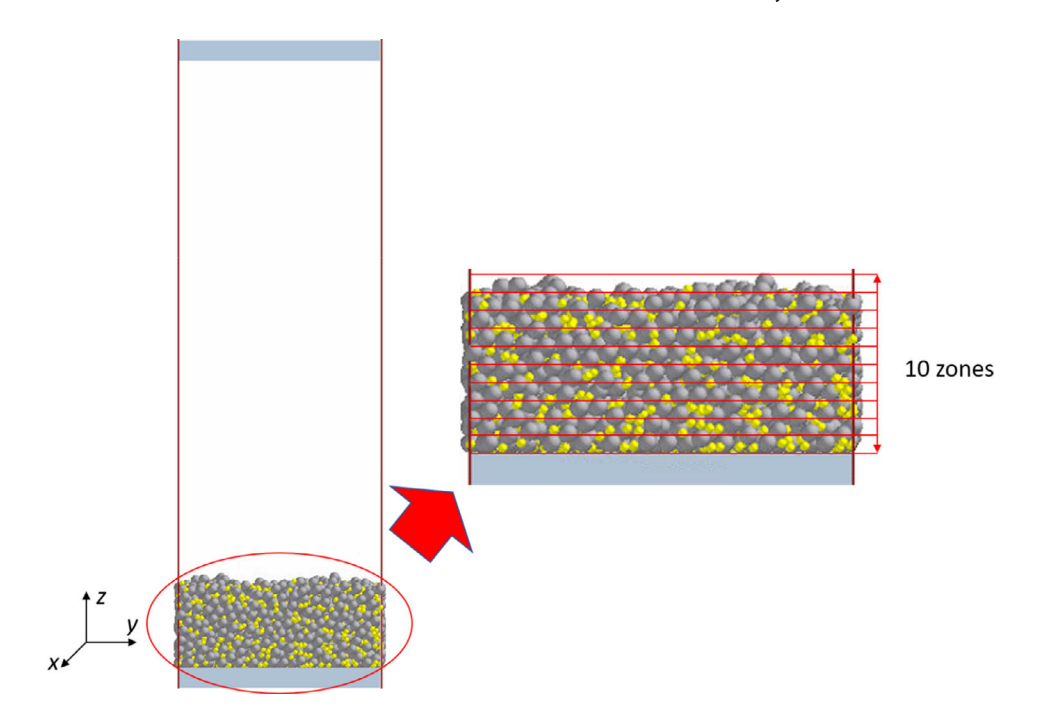
$$R_m = \frac{\Delta C_v}{t_h}.$$
 (11)

Here,  $\Delta C_{\rm v}$  is the change in the  $C_{\rm v}$  value compared to  $t=0\,{\rm s}$ , and  $t_h$  is the time to reach homogeneity or the endpoint of the process (10 s in this study). The collision rate is defined as the number of collisions per particle per second. Thus, the average collision rate is another important parameter for evaluating the mixing performance, which is defined below.

$$Collision_{rate} = \frac{\sum C_{n,i}}{t_{n*}N},$$
 (12)

where  $C_n$  is collision number (number of collisions per second) for each particle,  $t_c$  is collision time, and N is the number of particles. To facilitate predictive estimation of the mixing behavior in the

**FIGURE 2** Schematic (side view) of cohesive particles generated in high vibration system



high-intensity vibration system, a dimensionless mixing Bond number ( $Bo_m$ ) is introduced here. Mixing Bond number is defined as the ratio of the cohesive force (pull-off force), which could be calculated based on Equation (8), to the collision shear force.

$$Bo_m = \frac{F_{\text{pull off}}}{F_{\text{collision shear}}}.$$
 (13)

$$F_{\text{collision shear}} = -S_t \delta_t.$$
 (14)

$$S_t = 8G^* \sqrt{R_e \delta}. \tag{15}$$

Here,  $\delta_t$  is tangential overlap,  $S_t$  is the tangential stiffness, and  $G^*$  is the equivalent shear modulus. Because the aim of this study is to investigate the mixing behavior between fine and coarse particles, the Bond number is defined as in Equation (13) where the numerator accounts for the characteristic cohesion force, which if the pull-off force between fine and coarse particles, which is the force needed to break the most relevant particle interactions. The denominator is the system shear force, which accounts for the characteristic force that could counter cohesion. The system shear force is based on the coarse–coarse particle collisions, which are expected to be the most important type of collisions in the system. As will be explained later, thus, the average coarse–coarse particle collision shear force is used to capture the system collision force in the denominator of the equation.

# 3 | NUMERICAL RESULTS AND DISCUSSIONS

The effect of vibration intensity was investigated by varying the displacement magnitude from 5 to 10 mm, while keeping the frequency

(60 Hz) fixed. This allowed the mixing intensity to vary from 50 to 100 Gs. Hence, in this study, displacement amplitude can represent mixing intensity. Higher displacement amplitude equates to higher processing intensity or effective acceleration. Interparticle cohesive force is highly dependent on the particle size, van der Waals force, moisture, electrostatic and, capillary force, etc. In this study, the cohesive force is assumed to be the pull-off force based on the JKR model, which is related to the surface energy. Thus, by changing the value of the surface energy, the effect of cohesive forces on mixing quality could be investigated.

### 3.1 | Vibration intensity effect on mixing behavior

Mixing experiments of two sets of mono-sized particles (250 and 500  $\mu$ m) were conducted using the same surface energy (5 J/m<sup>2</sup>), while varying the processing amplitude from 5 to 10 mm. Figure 3 depicts the mixing performances after processing 1, 5, and 10 s at different processing intensities. It can be observed that, in all cases, the degree of mixing increased with the increase of mixing time, which means longer processing time leads to better mixing quality. In addition, the mixing rate, at high processing intensity, was much faster than that at low intensity. It is clear to see from Figure 3A that after 1 s, fine particles (yellow) transferred from top to bottom. On the other hand, Figure 3C shows that most fine particles were still on the top of coarse ones, even after processing for 10 s with 5 mm amplitude. While very qualitative, visual observation indicates that at higher amplitudes of 10 and 7.5 mm, a relatively high degree of homogeneity was achieved in 5 and 10 s, respectively. Meanwhile, this was not true for the 5-mm case. This is quantified in Figure 4, which depicts the  $C_v$ values of fine particles as a function of time at different processing intensities. In all cases, C<sub>v</sub> values reduced with increasing mixing time,

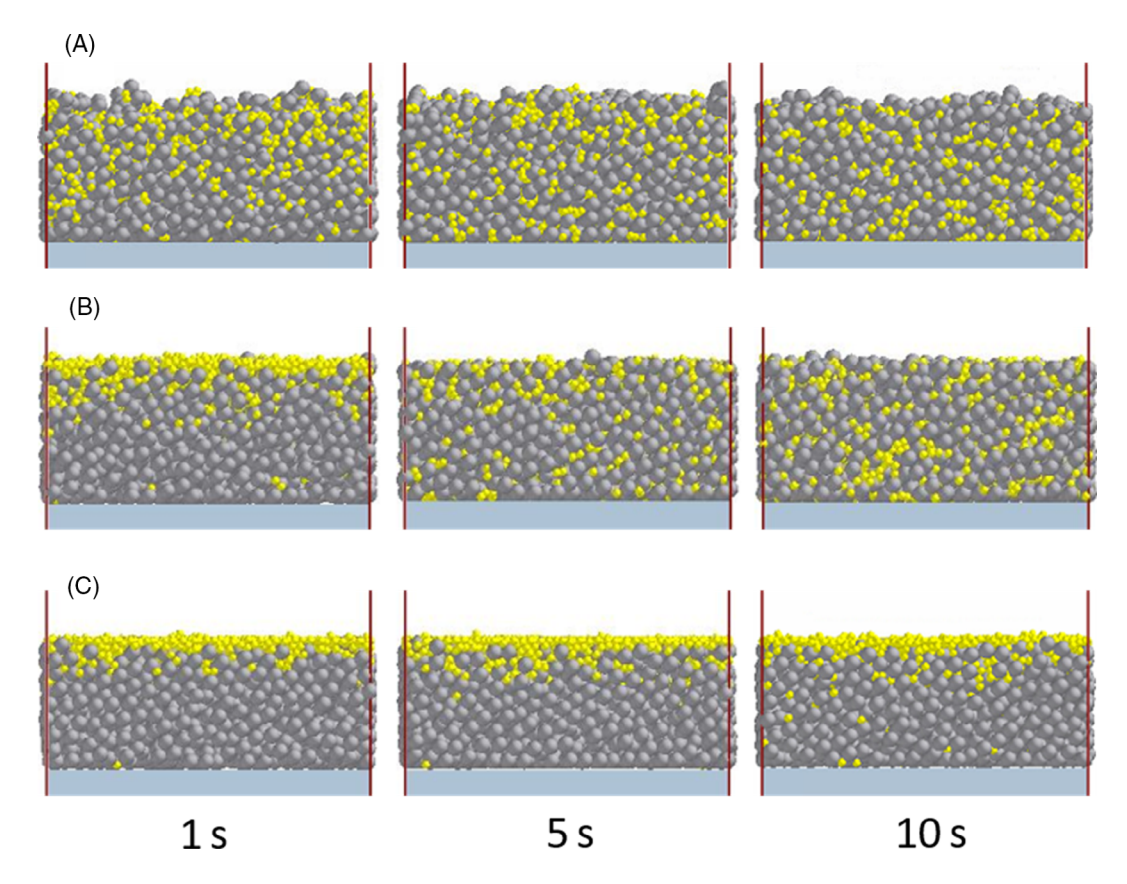
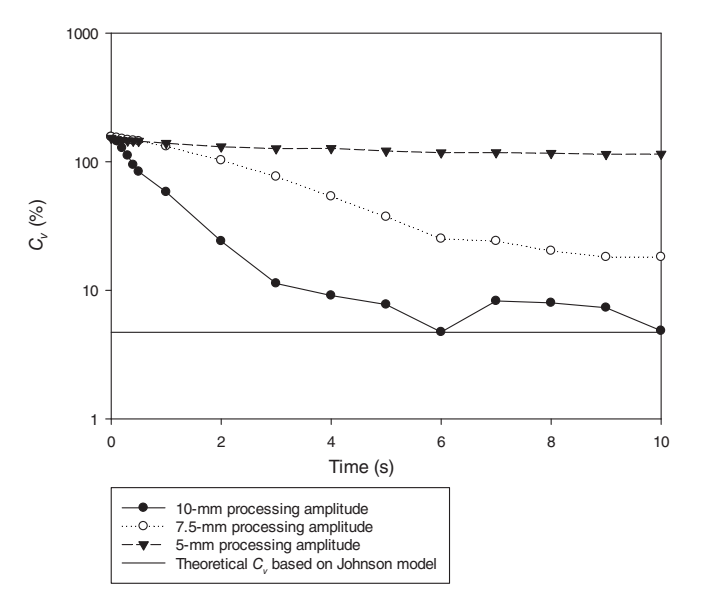


FIGURE 3 Mixing performances after processing 1, 5, and 10 s under processing amplitude of (A) 10 mm, (B) 7.5 mm, and (C) 5 mm

which was expected. The actual  $C_{\rm v}$  value reached the theoretical well-mixing  $C_{\rm v}$  value (4.7%) in 6 s, and maintained steady state for the next 4 s when using a processing amplitude of 10 mm, indicating particles were well mixed and no segregation or de-mixing phenomenon was observed.  $C_{\rm v}$  value reduced from 156% to 18.2% when processed at the 7.5-mm amplitude for 10 s. However, for the 5-mm amplitude case, the  $C_{\rm v}$  value only declined from 154% to 115%, and at a much slower rate as compared to the other two cases. For the 5- and 7.5-mm amplitude mixing cases, although  $C_{\rm v}$  values declined with the increase of processing time, 10 s was still not long enough to properly mix the particles at such intensities. Hence, longer processing time is suggested. In conclusion, high processing intensity could significantly elevate the mixing speed for cohesive powders. Similar phenomenon has also been reported in another work.<sup>57</sup>

# 3.2 | Effect of vibration intensity on collision shear force, collision rate, and particle bed porosity

In order to better understand why high intensity led to better mixing rate and quality, the mixing mechanism was further investigated. For high-intensity vibration-based mixing, particles randomly collide with each other. This type of random, collision-driven rearrangement has been reported as diffusion-like mixing. In the diffusion-like mixing process, the diffusion or mixing rate depends on the shear rate and particle size. 6.58 Since particles having identical properties were used in this study, the



**FIGURE 4** Coefficient of variation  $(C_v)$  values of fine particles as a function of time at various processing amplitudes

effective "viscosities" of mixtures are assumed to be the same. Mixing simulations for two sets of mono-sized particles (250 and 500  $\mu m)$  were performed using the same surface energy (5 J/m²) with processing amplitudes varied from 5 to 10 mm, and fixed processing time of 10 s. Collision shear force was obtained from EDEM, which depends on

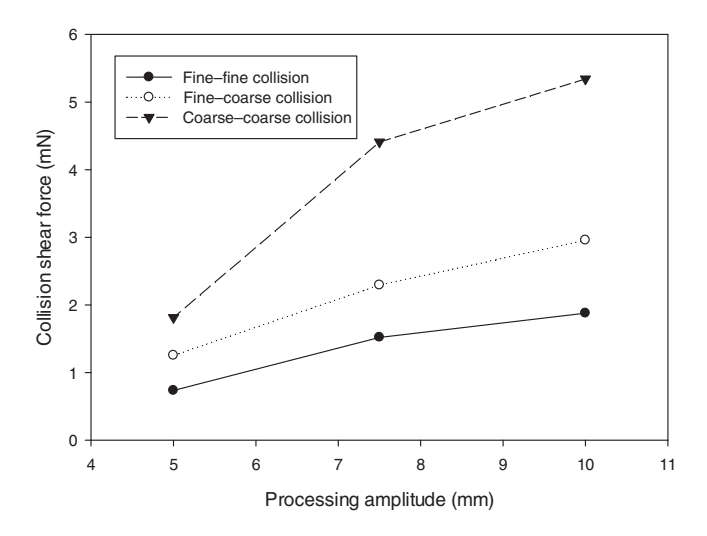


**FIGURE 5** Average collision shear force between fine-fine, fine-coarse, and coarse-coarse particles as a function of processing amplitude

tangential overlap and tangential stiffness, and is derived from the Mindlin-Deresiewicz theory. 59 Average collision number was evaluated to further assess the mixing process. Three types of particle collisions were considered: fine-fine, fine-coarse, and coarse-coarse. The particle collision force was calculated based on the average collision force computed through EDEM. Since too many collisions occurred simultaneously while the collision shear force changes at different time steps, averaging of particle collision shear force was required. Figure 5 displays the average collision shear force for collisions between fine-fine, fine-coarse, and coarse-coarse particles as a function of mixing intensity. The particle collision shear force for all three types of collisions increases as mixing intensity increased from 5 to 10 mm. This may be due to high-intensity mixing enhancing the relative velocities between the particles.<sup>49</sup> Thus, the dynamic assessment of the particle bed porosity is important, and more details will be discussed in the later section. In addition, the average collision force between coarse particles was far larger than the finefine and fine-coarse, as expected. An interesting finding is that the increase of collision shear force from the 7.5- to 10-mm amplitude case was much larger than that from 5 to 7.5 mm. This indicates the effect of processing intensity on collision shear force was nonlinear. This is because the collision shear force is related to the collision normal force, which is directly proportional to the square of the relative velocity between particles in the high-intensity vibration system.<sup>49</sup>

Figure 6 presents the effect of mixing intensity on collision rate for collisions between fine-fine, fine-coarse, and coarse-coarse particles. As shown, collision rate rose with increasing processing intensity for all three cases, thus indicating higher intensity would lead to faster mixing rate. An interesting finding is that the fine-fine particle collision rate was much smaller than that of fine-coarse and coarse-coarse collisions, indicating collisions involving coarse particles were dominant in high-intensity vibration systems. Both the average coarse-coarse collision shear force (Figure 5) and their collision rates (Figure 6) were higher than those of fine-fine and fine-coarse collisions, which means the

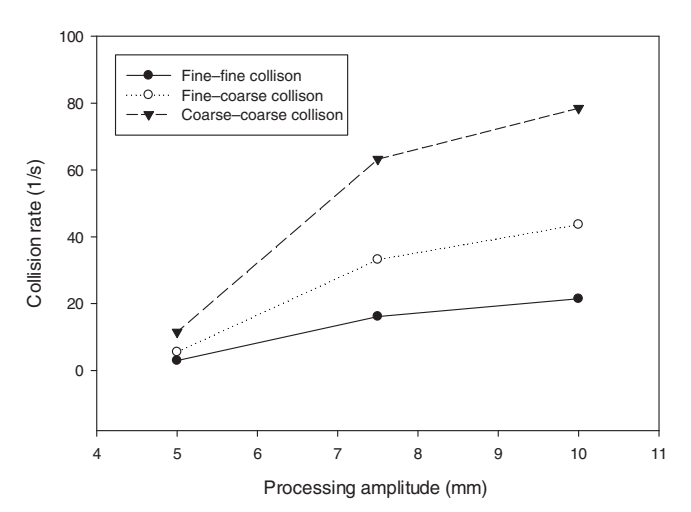


**FIGURE 6** Average collision rate between fine–fine, fine–coarse, and coarse–coarse particles as a function of processing amplitude

system is dominated by coarse–coarse particle collisions. The energy consumed for particle diffusion was mainly from coarse–coarse particle collision energy. Thus, it was found that the mixing performance was highly dependent on the collisions between coarse particles. Therefore, coarse–coarse collision shear force was used in the denominator to compute mixing Bond number in Equation (13) to facilitate predictive estimation of the mixing behavior.

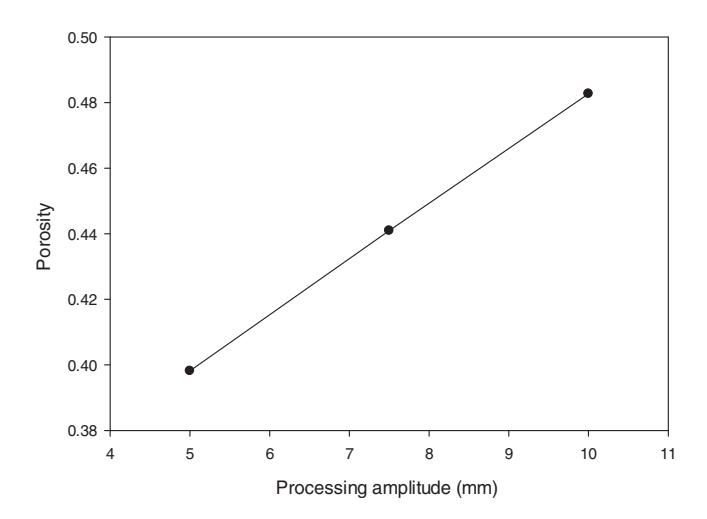
In the simulated high-intensity mixing system, the bed of particles has a tendency to move together as a whole; hence, the phenomena could be treated as a moving powder bed. Since porosity plays a significant role in the mixing process, 60 the effect of processing intensity on powder bed porosity was evaluated. Here, powder bed porosity is defined as the ratio of total pore volume to apparent volume of the moving powder bed and not the entire available vessel space. Figure 7 plots the powder bed porosity as a function of processing amplitude, which increased from 0.4 to 0.48, as processing amplitude increased from 5 to 10 mm. It has been reported that the mixing quality is dependent on powder bed porosity. 61,62 For example, displacement, wedging, and confinement effects are expected when fine particles percolate around the large particles. Therefore, if the porosity is higher, it affords a higher degree of motion, where the presence of more void space could facilitate higher levels of diffusion of finer particles, and reduce the effects due to constrained motions at lower porosity. In addition, it could enhance the mean free path of particles which leads to higher relative velocity and collision force that could overcome pull-off forces between particles. Both of these effects could help enhance the mixing rate. In conclusion, the higher processing intensity could enhance particle mixing rate by increasing particle collision shear forces, collision numbers, and powder bed porosities.

# 3.3 | Effect of surface energy on mixing behavior

The effect of cohesion on particle mixing was evaluated by investigating the maximum cohesion force or pull-off force. Since pull-off force

is related to surface energy, the effect of surface energy on particle mixing quality was investigated. Mixing experiments of two sets of mono-sized particles (250 and 500  $\mu m)$  were conducted using the same processing intensity (10 mm) with surface energy varied by two orders of magnitude from 0.5 to 50 J/m² for 10 s. The surface energy of 50 J/m² was regarded as a very cohesive case and 0.5 J/m² was regarded as a nearly noncohesive case.

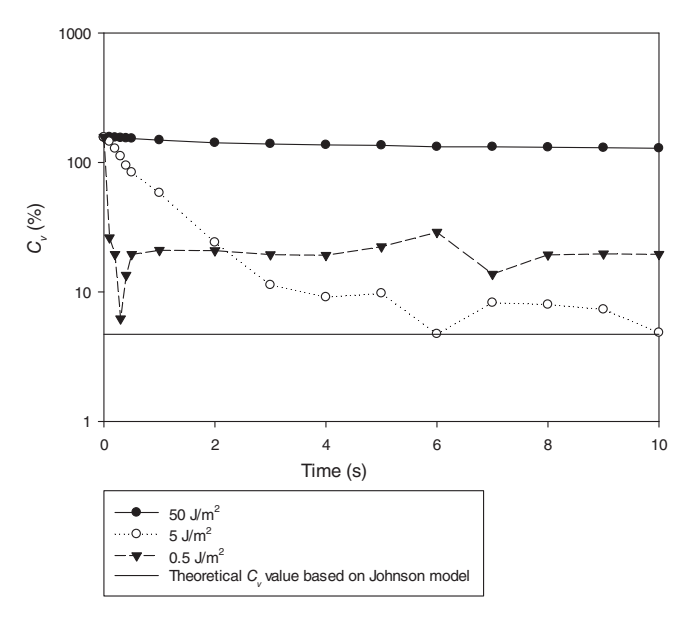
Figure 8 depicts the  $C_v$  values of fine particles as a function of time at different surface energy values, all processed at a processing amplitude of 10 mm. It can be observed that the  $C_v$  value decreased



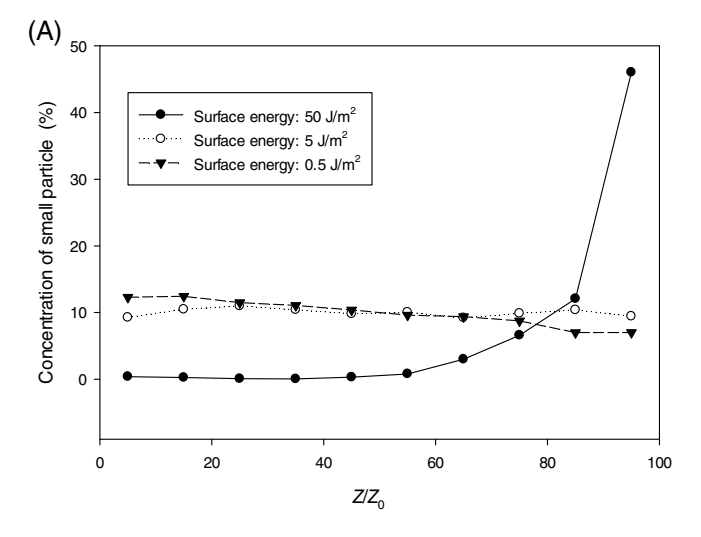
**FIGURE 7** Powder bed porosity as a function of processing amplitude

(B)

faster with decreasing surface energy. For the  $0.5 \, \text{J/m}^2$  case, the  $C_v$  value reduced to the theoretical well-mixing  $C_v$  value (4.7%) in  $0.3 \, \text{s}$ . Unfortunately, it then elevated to 20% after  $0.5 \, \text{s}$ , which was likely due to the de-mixing or segregation of particles upon further shear. On the other hand, the  $C_v$  value only reduced from 157% to 115% after 10 s when surface energy was very high (50  $\, \text{J/m}^2$ ). A similar



**FIGURE 8** Coefficient of variation  $(C_v)$  values of fine particles as a function of time. Various surface energy values were used, and processing amplitude was set at the highest level of 10 mm



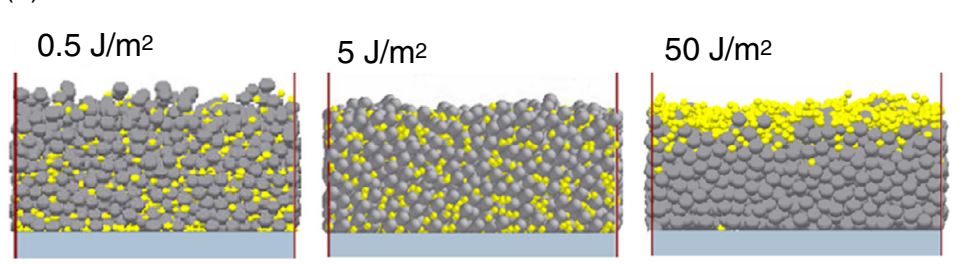
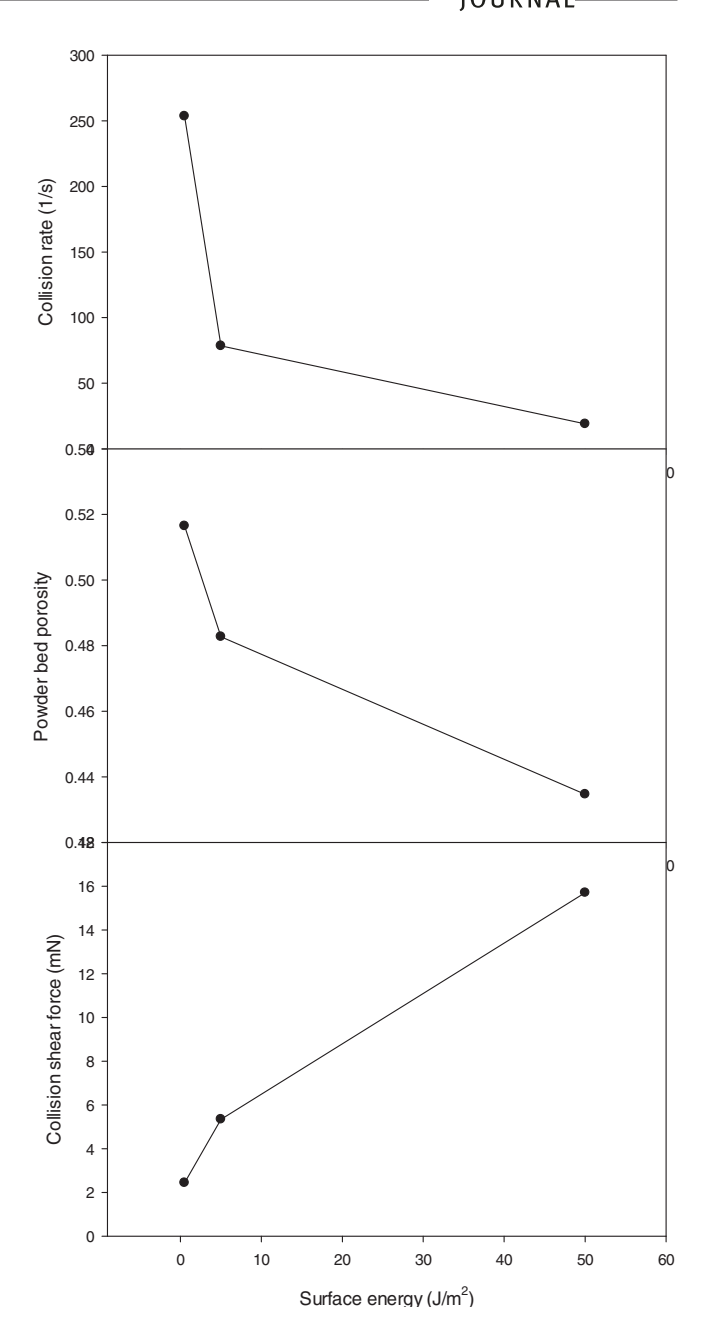


FIGURE 9 (A) Fine particle concentration as a function of vertical axis at 10 s under the highest processing amplitude of 10 mm, (B) side view

experimental observation was also made in our previous study that the homogeneity of noncohesive dry coated particles first reduced and then increased.<sup>4</sup> In that work, the C<sub>v</sub> values for 3% and 5% active pharmaceutical ingredient (API) loaded blends reached the desired level when mixing time was 40 min. The  $C_v$  values at 40 min were lower than those when mixing times were 10 and 90 min. Such experimental results corroborate the current observations from DEM simulations. Similarly, it was also found that high processing intensity was not always beneficial for mixing,<sup>49</sup> because blends achieved better homogeneity when processed at 30 Gs instead of 90 Gs. Such experimental results corroborate with the DEM simulation results. Therefore, it can be said that either too high or too low values of surface energy or cohesion force are not good for achieving very good mixing, which was also observed in previous research.<sup>4,6,9</sup> Hence, it is likely that high cohesion force reduces mixing rate while low cohesion force leads to particle segregation.

Figure 9 presents the concentration of fine particles as a function of vertical axis at 10 s under a processing amplitude of 10 mm. In this figure, the normalized distance (z axis) of 0 is the bottom of the container, and 100 is the top of powder bed. In the intermediate surface energy case ( $5 \text{ J/m}^2$ ), fine particles were well mixed after 10 s. However, in the low surface energy case ( $0.5 \text{ J/m}^2$ ), the concentration of fine particles decreased with increasing powder bed height. This means more fine particles transferred from the top to bottom, indicating segregation of particles occurred. However, in the high surface energy case ( $50 \text{ J/m}^2$ ), the concentration of fine particles rose with increasing powder bed height, which means most of the fine particles stayed on top of the powder bed.

To further analyze the mixing mechanism, collision shear force, collision rate, and powder bed porosity were described as functions of surface energy. Since the mixing system is dominated by coarsecoarse particle collisions, and the trend of collision shear force and collision rate are similar for the various particle collision types, it is sufficient to only examine the coarse-coarse particle collisions. Figure 10 displays collision shear force, collision rate, and porosity as a function of surface energy at the highest processing amplitude of 10 mm and processing time of 10 s. It is observed that the coarsecoarse particle collision shear force rose from 2.4 to 15.7 mN with increase of surface energy from 0.5 to 50 J/m<sup>2</sup>, which in principle could enhance the mixing rate and improve the homogeneity of the mixture. However, both the collision rate and particle bed porosity decreased; collision rate decreased from 253 to 19 1/s and particle bed porosity decreased from 0.52 to 0.43 with an increase of surface energy from 0.5 to 50 J/m<sup>2</sup>. Since higher surface energy leads to much higher pull-off force between fine-coarse and coarse-coarse particles, it is much more difficult to break the contacts of particles. That leads to less free particles, which leads to lower collision rate. In addition, since higher surface energy particles tend to stick together, the particles are expected to pack more tightly during the mixing process.<sup>49</sup> Therefore, even when the large collision shear force helps improve the mixing rate, it was not high enough to overcome the effect of low collision rate and low powder bed porosity. Such results were evident from Figures 9 and 10. In conclusion, very high cohesion



**FIGURE 10** Collision rate, powder bed porosity, and collision shear force as a function of surface energy

force between particles is not desired for powder mixing. This aspect could explain why dry powder coating could enhance the mixing quality by reducing the cohesive force between fine particles.<sup>4</sup>

# 3.4 | Ratio of cohesive force to collision shear force

As mentioned in previous sections, mixing rate and mixing quality are significantly affected by particle collision shear force, number of collisions, and powder bed porosity. However, results so far have not produced a simple way to predict mixing rate and mixing quality because

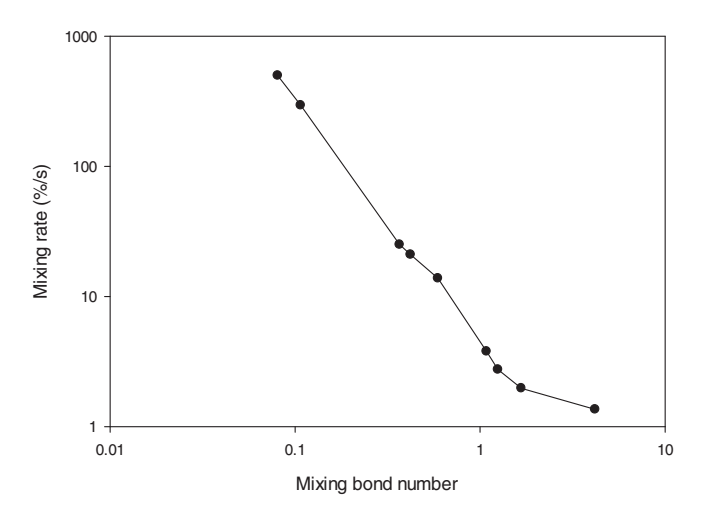


**FIGURE 11** Effective mixing rate as a function of mixing Bond number

of the multiple factors that are involved, including process intensity and time. Thus, mixing Bond number was introduced, and can be calculated using Equation (13). Based on Equation (13), if the average shear force is higher than the pull-off force between particles, it leads to a faster mixing rate. The mixing experiments were conducted using two sets of mono-sized particles (250 and 500  $\mu m$ ), along with two processing intensities (5 and 10 mm), and two surface energies (0.5 and 50 J/m²) for 10 s.

Figure 11 presents effective mixing rate as a function of mixing Bond number. It was found that mixing rate declined with increasing mixing Bond number, indicating higher cohesive force to collision shear force ratio is not good for mixing. The highest mixing rate 499%/s was observed when the particle mixture with surface energy of 0.5 J/m<sup>2</sup> was mixed at 10 mm amplitude. On the other hand, the lowest mixing rate 1.36%/s was observed when the particle mixture with surface energy of 50 J/m<sup>2</sup> was mixed at 5 mm amplitude, implying these parameters lead to the lowest mixing intensity. This led to the lowest mixing Bond number as well, indicating that collision shear force is not large enough to overcome the cohesive force between particles. Both simulations validated the observation that low cohesion force and high processing intensity enhance the mixing rate. However, as high mixing rate does not always lead to good mixing quality, the mixing time is another parameter in the particle mixing process. It is noted that in general, collision shear forces of both the coarse-coarse and fine-coarse collisions increase with the increasing intensity as seen in Figure 5. Therefore, it is reasonable to use coarse-coarse collision forces in Equation (13) although the general trend and conclusion would be the same if fine-coarse collision forces are used in Equation (13), albeit the force magnitudes would be different. Figure 12 describes the  $C_v$  values of fine particles as a function of the product  $(P_{r,t})$  of effective mixing rate and mixing time. It was found that  $C_v$  values initially decreased, and then rose with an increase in the product of effective mixing rate and mixing time. The minimum  $C_v$ value was observed when  $P_{r,t}$  is around 100% to 300%. As shown in Figure 12, when  $P_{r,t}$  value was very small, it is found that the  $C_v$  value

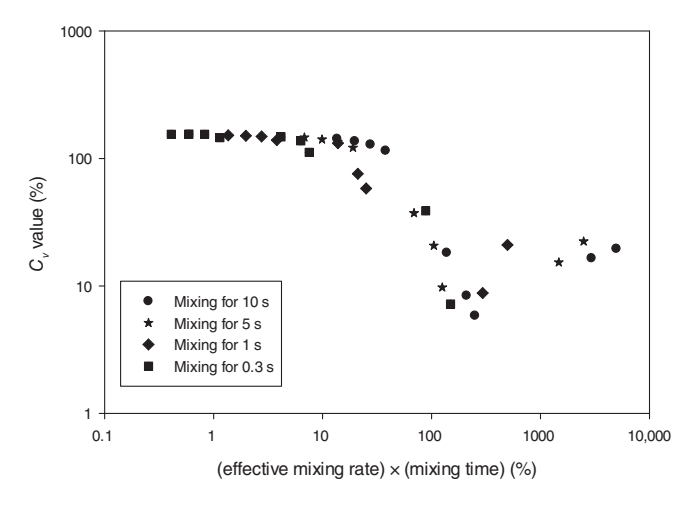


**FIGURE 12** Coefficient of variation  $(C_v)$  values of fine particles as a function of the product of effective mixing rate and mixing time

was relatively high, which means mixing was not sufficient and mixing quality will not be as good as expected. On the other hand, when  $P_{rt}$ was very high, although mixing rate was very fast and the processing time was long, segregation of particles was observed during the mixing process and adequate mixing quality was not attained. Both very high or very low values of  $P_{r,t}$  lead to inadequate mixing. These simulation results are in line with similar experimental observations from a previous work, where, as the mixing time increased, the homogeneity of blends of larger free-flowing excipients with finer drug powders, which became noncohesive after dry coating, first reduced, and then increased.<sup>4,24</sup> That was attributed to potential segregation driven by disparate sizes of the powder constituents. Another experimental and modeling study demonstrated that higher mixing intensity could lead to poorer dry coating, which is also similar to ordered mixing.<sup>49</sup> These studies support the current findings that processing intensity and time are critical factors in mixing along with the cohesion.

# 4 | CONCLUSION

The cohesive particle mixing process for binary blends in a high-intensity vibration system was investigated via DEM simulations. Analysis of the collision shear force, collision rate, and powder bed porosity as a function of particle size, mixing intensity, particle cohesion, and processing time helped reveal the mixing dynamics and mechanism. When processed at the highest mixing intensity used in this study, the coefficient of variation,  $C_v$ , reached the theoretical well-mixed  $C_v$  value (4.7%) in 6 s, indicating particles were well mixed. This well-mixed state was also maintained for the remainder of the simulation time. It was found that the mixing process is dominated by coarse–coarse particle collisions. High processing intensity enhances collision shear forces and collision rates, which increase powder bed porosity and result in a higher mixing rate. Thus, high processing intensity is recommended to enhance the mixing efficiency when

AICHE 11 of 12

powders are cohesive. In addition, the effect of cohesion on particle mixing was evaluated by varying surface energy. C<sub>v</sub> value reduced to theoretical well-mixed value (4.7%) in 0.3 s and then rose to 20% after 0.5 s when particles had the low surface energy value of 0.5 J/m<sup>2</sup>. On the other hand, C<sub>v</sub> value only reduced from 157% to 115% at 10 s with a very high surface energy of 50 J/m<sup>2</sup>. Such complex mixing dynamics were captured through introduction of a dimensionless parameter, termed the mixing Bond number (Bom), to predict the effective mixing rate, R<sub>m</sub>. The effective mixing rate was found to be inversely related to  $Bo_m$ . Finally, the product of the effective mixing rate and mixing time  $(P_{r,t})$  was used to characterize the mixing behavior. It was found that ideal mixing occurs when  $P_{r,t}$  was just above the value of 100%. However, both too high or too low  $P_{r,t}$  values, resulting from too high or too low cohesion force or surface energy, are not conducive to proper mixing. If  $P_{r,t}$  is too low, mixing is insufficient. If  $P_{r,t}$  is too high, even when the mixing rate could be fast, segregation of particles may occur since mixing time would be long. Overall, if the powder is very cohesive, high processing intensity and long processing time would be required to reach mixture homogeneity. Meanwhile, if the powder is free flowing or weakly cohesive, a lower processing intensity and shorter processing time would be preferred for achieving adequate mixing quality.

#### **ACKNOWLEDGMENT**

The authors gratefully acknowledge partial financial support from the National Science Foundation (NSF) through grant IIP-1919037.

#### **AUTHOR CONTRIBUTIONS**

Kai Zheng: Investigation (equal); methodology (equal); writing – original draft (equal). Kuriakose Kunnath: Writing – review and editing (supporting). Rajesh N. Davé: Supervision (equal); writing – review and editing (equal).

### DATA AVAILABILITY STATEMENT

The data that support the findings of this study are available from the corresponding author upon reasonable request.

#### ORCID

Rajesh N. Davé https://orcid.org/0000-0001-7706-2259

#### **REFERENCES**

- Kwant G, Prins W, van Swaaij WPM. Particle mixing and separation in a binary solids floating fluidized bed. Powder Technol. 1995;82(3):279-291.
- Alonso M, Alguacil F. Dry mixing and coating of powders. Rev Metal. 1999;35:315-328
- Asachi M, Nourafkan E, Hassanpour A. A review of current techniques for the evaluation of powder mixing. Adv Powder Technol. 2018;29(7):1525-1549.
- Huang Z, Xiong W, Kunnath K, Bhaumik S, Davé RN. Improving blend content uniformity via dry particle coating of micronized drug powders. Eur J Pharm Sci. 2017:104:344-355.
- Kunnath K, Huang Z, Chen L, Zheng K, Davé R. Improved properties of fine active pharmaceutical ingredient powder blends and tablets at high drug loading via dry particle coating. Int J Pharm. 2018;543(1): 288-299.

- Fry A, Umbanhowar P, Ottino J, Lueptow R. Diffusion, mixing, and segregation in confined granular flows. AIChE J. 2019;65:875-881.
- Weinekötter R, Gericke H. Equipment for mixing of solids. In: Weinekötter R, Gericke H, eds. Mixing of Solids. Springer Netherlands; 2000:55-65.
- Chaudhuri B, Mehrotra A, Muzzio FJ, Tomassone MS. Cohesive effects in powder mixing in a tumbling blender. *Powder Technol*. 2006; 165(2):105-114.
- Deng X, Zheng K, Davé RN. Discrete element method based analysis of mixing and collision dynamics in adhesive mixing process. Chem Eng Sci. 2018;190:220-231.
- Savage SB, Lun CKK. Particle size segregation in inclined chute flow of dry cohesionless granular solids. J Fluid Mech. 1988;189:311-335.
- Ottino JM, Khakhar DV. Mixing and segregation of granular materials. Annu Rev Fluid Mech. 2000;32(1):55-91.
- Moes JJ, Ruijken MM, Gout E, Frijlink HW, Ugwoke MI. Application of process analytical technology in tablet process development using NIR spectroscopy: blend uniformity, content uniformity and coating thickness measurements. *Int J Pharm.* 2008;357(1-2): 108-118.
- Gao Y, Vanarase A, Muzzio F, Ierapetritou M. Characterizing continuous powder mixing using residence time distribution. *Chem Eng Sci.* 2011;66(3):417-425.
- Portillo PM, Ierapetritou MG, Muzzio FJ. Effects of rotation rate, mixing angle, and cohesion in two continuous powder mixers—a statistical approach. *Powder Technol*. 2009;194(3):217-227.
- Samadani A, Kudrolli A. Segregation transitions in wet granular matter. Phys Rev Lett. 2000;85(24):5102-5105.
- Khakhar DV, McCarthy JJ, Ottino JM. Mixing and segregation of granular materials in chute flows. Chaos. 1999;9(3):594-610.
- Alonso M, Satoh M, Miyanami K. Mechanism of the combined coating-mechanofusion processing of powders. *Powder Technol*. 1989:59(1):45-52.
- Pfeffer R, Dave RN, Wei D, Ramlakhan M. Synthesis of engineered particulates with tailored properties using dry particle coating. *Powder Technol*. 2001;117(1):40-67.
- Bertrand F, Leclaire LA, Levecque G. DEM-based models for the mixing of granular materials. Chem Eng Sci. 2005;60(8):2517-2531.
- Castellanos A. The relationship between attractive interparticle forces and bulk behaviour in dry and uncharged fine powders. Adv Phys. 2005;54(4):263-276.
- Li Q, Rudolph V, Peukert W. London-van der Waals adhesiveness of rough particles. Powder Technol. 2006;161:248-255.
- 22. Chen Y, Yang J, Dave RN, Pfeffer R. Fluidization of coated group C powders. AIChE J. 2008;54(1):104-121.
- Yang J, Sliva A, Banerjee A, Dave RN, Pfeffer R. Dry particle coating for improving the flowability of cohesive powders. *Powder Technol*. 2005;158(1):21-33.
- Huang Z, Scicolone JV, Gurumuthy L, Davé RN. Flow and bulk density enhancements of pharmaceutical powders using a conical screen mill: a continuous dry coating device. Chem Eng Sci. 2015;125:209-224.
- Chen L, Ding X, He Z, et al. Surface engineered excipients:
  I. improved functional properties of fine grade microcrystalline cellulose. Int J Pharm. 2018;536(1):127-137.
- Harnby N, Edwards MF, Nienow AW. Mixing in the Process Industries.
  2nd ed. Butterworth-Heinemann; 1997.
- Deng X, Scicolone JV, Davé RN. Discrete element method simulation of cohesive particles mixing under magnetically assisted impaction. Powder Technol. 2013;243:96-109.
- Muzzio FJ, Llusa M, Goodridge CL, Duong N-H, Shen E. Evaluating the mixing performance of a ribbon blender. *Powder Technol*. 2008; 186(3):247-254.
- Ding YL, Seville JPK, Forster R, Parker DJ. Solids motion in rolling mode rotating drums operated at low to medium rotational speeds. Chem Eng Sci. 2001;56(5):1769-1780.

- Moakher M, Shinbrot T, Muzzio FJ. Experimentally validated computations of flow, mixing and segregation of non-cohesive grains in 3D tumbling blenders. *Powder Technol.* 2000;109(1-3):58-71.
- Porion P, Sommier N, Faugère AM, Evesque P. Dynamics of size segregation and mixing of granular materials in a 3D-blender by NMR imaging investigation. *Powder Technol.* 2004;141(1-2):55-68.
- Dave R, Chen W, Mujumdar A, Wang W, Pfeffer R. Numerical simulation of dry particle coating processes by the discrete element method. Adv Powder Technol. 2003;14(4):449-470.
- Huang Z, Scicolone JV, Han X, Davé RN. Improved blend and tablet properties of fine pharmaceutical powders via dry particle coating. Int J Pharm. 2015;478(2):447-455.
- Fan H, Guo D, Dong J, Cui X, Zhang M, Zhang Z. Discrete element method simulation of the mixing process of particles with and without cohesive interparticle forces in a fluidized bed. *Powder Technol*. 2018;327:223-231.
- Deng X, Scicolone J, Han X, Davé RN. Discrete element method simulation of a conical screen mill: a continuous dry coating device. Chem Eng Sci. 2015;125:58-74.
- Escotet-Espinoza M, Foster CJ, Ierapetritou M. Discrete element modeling (DEM) for mixing of cohesive solids in rotating cylinders. Powder Technol. 2018;335:124-136.
- Zhu HP, Zhou ZY, Yang RY, Yu AB. Discrete particle simulation of particulate systems: a review of major applications and findings. *Chem Eng Sci.* 2008;63(23):5728-5770.
- Zhu HP, Zhou ZY, Yang RY, Yu AB. Discrete particle simulation of particulate systems: theoretical developments. *Chem Eng Sci.* 2007; 62(13):3378-3396.
- Lemieux M, Bertrand F, Chaouki J, Gosselin P. Comparative study of the mixing of free-flowing particles in a V-blender and a bin-blender. Chem Eng Sci. 2007;62(6):1783-1802.
- Portillo PM, Muzzio FJ, Ierapetritou MG. Hybrid DEM-compartment modeling approach for granular mixing. AIChE J. 2007;53(1):119-128.
- 41. Sarkar A, Wassgren CR. Effect of particle size on flow and mixing in a bladed granular mixer. AIChE J. 2015;61(1):46-57.
- 42. Hou QF, Dong KJ, Yu AB. DEM study of the flow of cohesive particles in a screw feeder. *Powder Technol.* 2014;256:529-539.
- 43. Johnson KL, Kendall K, Roberts AD. Surface energy and contact of elastic solids. *Proc R Soc A Math Phys Eng Sci.* 1971;324:301-313.
- Mindlin RD. Elastic spheres in contact under varying oblique forces. J Appl Mech. 1953;1953(20):327-344.
- 45. Thornton C, Yin KK. Impact of elastic spheres with and without adhesion. *Powder Technol.* 1991;65(1):153-166.
- Liu G, Li S, Yao Q. A JKR-based dynamic model for the impact of micro-particle with a flat surface. *Powder Technol.* 2011;207(1): 215-223.
- 47. Hærvig J, Kleinhans U, Wieland C, et al. On the adhesive JKR contact and rolling models for reduced particle stiffness discrete element simulations. *Powder Technol.* 2017;319:472-482.

- 48. Barthel E. Adhesive elastic contacts: JKR and more. J Phys D Appl Phys. 2008;41(16):163001.
- Zheng K, Kunnath K, Ling Z, Chen L, Davé RN. Influence of guest and host particle sizes on dry coating effectiveness: when not to use high mixing intensity. *Powder Technol*. 2020;366:150-163.
- 50. Nase S, Vargas W, Abatan A, McCarthy J. Discrete characterization tools for wet granular media. *Powder Technol.* 2001;116:214-223.
- Alexander AW, Chaudhuri B, Faqih A, Muzzio FJ, Davies C, Tomassone MS. Avalanching flow of cohesive powders. *Powder Technol*. 2006;164(1):13-21.
- Arratia PE, Duong N, Muzzio FJ, Godbole P, Reynolds S. A study of the mixing and segregation mechanisms in the Bohle Tote blender via DEM simulations. *Powder Technol*. 2006;164(1):50-57.
- 53. Džiugys A, Navakas R. The role of friction in mixing and segregation of granular material. *Granular Matter*. 2009;11(6):403-416.
- Gu Y, Ozel A, Sundaresan S. A modified cohesion model for CFD-DEM simulations of fluidization. *Powder Technol.* 2016;296:17-28.
- Song X, Zhang G. The role of the friction coefficients in the granular segregation in small systems. *Powder Technol*. 2020;372:40-47.
- Johnson MC. Particle size distribution of the active ingredient for solid dosage forms of low dosage. *Pharm Acta Helv.* 1972;47(8):546-559.
- Menbari A, Hashemnia K. Effect of vibration characteristics on the performance of mixing in a vertically vibrated bed of a binary mixture of spherical particles. Chem Eng Sci. 2019;207:942-957.
- Hsiau SS, Hunt ML. Shear-induced particle diffusion and longitudinal velocity fluctuations in a granular-flow mixing layer. J Fluid Mech. 1993;251:299-313.
- Ramírez-Aragón C, Ordieres-Meré J, Alba-Elías F, González-Marcos A. Comparison of cohesive models in EDEM and LIGGGHTS for simulating powder compaction. *Materials*. 2018;11(11):2341.
- Mota M, Teixeira J, Bowen W, Yelshin A. Binary spherical particle mixed beds: porosity and permeability relationship measurement. *Trans Filtr Soc.* 2001:1:101-106.
- Dias RP, Teixeira JA, Mota MG, Yelshin Al. Particulate binary mixtures: dependence of packing porosity on particle size ratio. *Ind Eng Chem Res*. 2004;43(24):7912-7919.
- Yu AB, Standish N. Estimation of the porosity of particle mixtures by a linear-mixture packing model. *Ind Eng Chem Res.* 1991;30(6):1372-1385.

**How to cite this article:** Zheng K, Kunnath K, Davé RN. Discrete element method simulation of binary blend mixing of cohesive particles in a high-intensity vibration system. *AIChE J.* 2022;68(4):e17603. doi:10.1002/aic.17603